Results: The four curves B, C, D and E in Fig. 1 are the transmission spectra of an LPG with a phase shift of 0, 0.5π, π and 1.5π, respectively. The other parameters of the grating areas follows: index change = 0.001, grating period = 696μm, grating length = 38.15nm. From the Figure we can see that with the increase in phase shift, the amplitude of the dip at the long wavelength side decreases, with its centre moving away from the central wavelength λ = 1550nm, and the dip at the short wavelength side increases, with its centre moving toward the central wavelength.

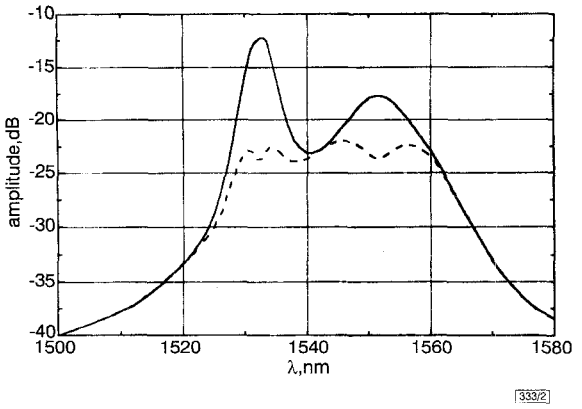

Fig. 2 *Unflattened and flattened spectra of Er:silica superfluorescent fibre source*

——— unflattened
– – – – flattened

The solid line in Fig. 2 shows the experimental spectrum of an Er:silica superfluorescent fibre source. The dotted line shows the expected output after using the phase-shifted LPG to flatten the gain spectrum. The flattened spectrum has a bandwidth > 30nm and a fluctuation < 2dB. The LPG used here is designed as follows: phase shift = 1.22π, index change = 0.0013, grating period = 684μm, grating length = 32.3mm. In designing the LPG, we first decide the grating period according to the phase matching condition, then decide the index change and grating length according to the bandwidth and amplitude of the gain spectrum. Finally, we choose a suitable phase shift to tailor the shape of the LPGs spectrum to fit the two peaks in the gain spectrum.

Conclusions: An efficient gain-flattening filter, designed using the phase-shifted long period grating, was presented. This kind of device can be designed to fit varying shapes of gain spectrum by choosing different phase shifts. It can flatten not only the spectrum of an erbium-doped fibre source, but also other erbium gain spectrums. Since the filter is realised with only one grating, it has the advantage of easy fabrication and thus has potential application in gain-flattening in WDM systems.

10 March 1998
Electronics Letters Online No: 19980768

J.R. Qian and H.F. Chen (*Optical Fiber Laboratory, Department of Electronic Engineering and Information Science, University of Science and Technology of China, PO Box 4, Hefei, Anhui, 230027, People's Republic of China*)

E-mail: jrqian@eeis.ustc.edu.cn, chf1027@eeis.ustc.edu.cn

References

1 WYSOCKI, P.F., JUDKINS, J.B., ESPINDOLA, R., ANDREJCO, M., VENGSARKAR, A.M., and WALKER, K.: 'Erbium-doped fiber amplifier flattened beyond 40nm using long-period grating'. Proc. Conf. Optic. Fiber Commun., OFC '97, 1997, paper PD2

2 WILKINSON, M., BEBBINGTON, A., CASSIDY, S.A., and MCKEE, P.: 'D-fibre filter for erbium gain spectrum flattening', *Electron. Lett.*, 1992, **28**, pp. 131–132

3 VENGSARKAR, A.M., PEDRAZZANI, J.R., JUDKINS, J.B., LEMANRE, P.J., BERGANO, N.S., and DAVIDSON, C.R.: 'Long-period fiber-grating-based gain equalizers', *Opt. Lett.*, 1996, **21**, pp. 336–338

4 NARAYANAN, C., PRESBY, H.M., and VENGSARKAR, A.M.: 'Band-rejection fibre filter using periodic core deformation', *Electron. Lett.*, 1997, **33**, pp. 280–281

5 HILL, K.O., MALO, B., VINEBERG, K., BILODEAU, F., JOHNSON, D., and SKINNER, I.: 'Efficient mode conversion in telecommunication fibre using externally written gratings', *Electron. Lett.*, 1990, **26**, pp. 1270–1272

6 BILODEAU, F., HILL, K.O., MALO, B., JOHNSON, D., and SKINNER, I.: 'Efficient narrowband LP01–LP02 mode convertors fabricated in photosensitive fibre: Spectral response', *Electron. Lett.*, 1991, **27**, pp. 682–684

7 VENGSARKAR, A.M., LEMAIRE, P.J., JACOBOVITZ-VESELKA, G., BHATIA, V., and JUDKINS, J.B.: 'Long-period fiber gratings as gain-flattening and laser stabilizing devices'. Proc. IOOC '95, June 1995, Hong Kong, postdeadline paper PD1–2

8 VENGSARKAR, A.M., LEMAIRE, P.J., JUDKINS, J.B., ITHATIA, V., ERDOGAN, T., and SIPE, J.E.: 'Long-period fiber gratings as band-rejection filters and spectral shape-shifters'. OFC '95, OSA Tech. Dig. Series, 1995, Vol. 8, paper PD4

9 UNGER, H.G.: 'Planar optical waveguides and fibres' (Clarendon, Oxford, 1997)

10 SNYDER, A.W., and LOVE, J.D.: 'Optical waveguide theory' (Chapman and Hall, London, 1984)

Metal-coated fibre Bragg grating sensor for electric current metering

P.M. Cavaleiro, F.M. Araújo and A.B. Lobo Ribeiro

A hybrid fibre optic current sensor combining a metal-coated fibre Bragg grating with a standard current transformer is described. Measurements of the RMS current of power lines at 50Hz with a resolution of 2mA is demonstrated.

The use of optical fibres as sensing elements for electric current measurement has been developed by several methods such as those utilising a magnetic field to generate the Faraday effect [1], magnetomotive force to make fibres bend [2], magnetostrictive material bonded on a fibre to constrict or lengthen the fibre [3], and heating effects to change the length and refractive index of fibres [3]. Recently, it has been shown that a system employing a fibre Bragg grating (FBG) bonded to a piezoelectric transducer (PZT) [4] can be constructed to measure alternating currents. There are, however, several disadvantages associated with the PZT scheme: (i) comparatively high voltages must be applied to the PZT; (ii) PZTs are fairly bulky and their frequency response is limited by circumferential resonance; (iii) the scheme requires a calibrated shunt resistor ('burner') which will considerably increase the cost of the system. This Letter describes a current sensor device based on the temperature sensitivity of a fibre Bragg grating. The temperature induced Bragg wavelength change is accomplished by passing electric current through a thin conductive coating on the surface of a short length of the fibre where the FBG is located.

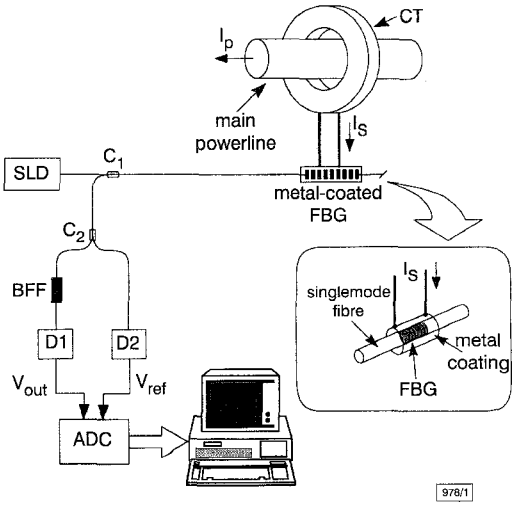

Fig. 1 *Schematic design of fibre optic current sensor*

The configuration of the optical fibre current sensor system is shown in Fig. 1. A pigtailed superluminescent diode (Superlum

SLD 361), emitting at 830nm with ~2mW optical power and ~20nm linewidth, was used to illuminate the metal-coated FBG via one port of a standard 3dB fibre coupler (C_1). The inset box of Fig. 1 depicts the FBG with a Bragg wavelength of ~836nm at room temperature (reflectivity ≈ 85%, bandwidth ≈ 0.3nm), coated with a ~1.4mm layer of low ion conductive pure silver epoxy. Electrical contacts were made at both ends of the coated region (typically 2cm long and having a ~1.2Ω resistance). The

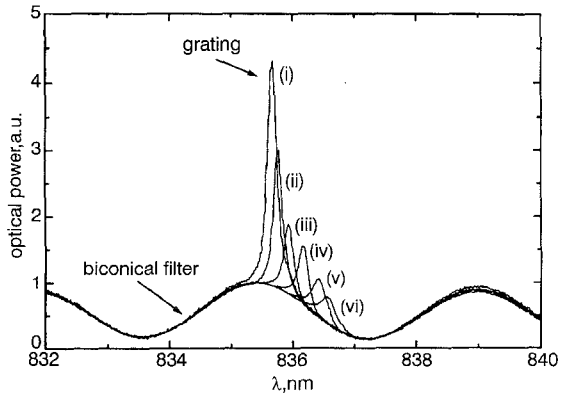

Fig. 2 *Biconical fibre filter transfer function superimposed with FBG spectra for different values of secondary current*

(i) I_S = 0A
(ii) I_S = 0.47A
(iii) I_S = 0.80A
(iv) I_S = 1.11A
(v) I_S = 1.47A
(vi) I_S = 1.60A

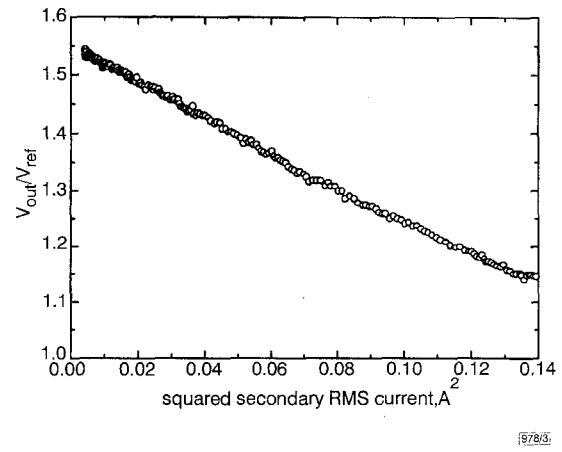

Fig. 3 *Output of sensor to applied alternating secondary current with frequency = 50Hz against square of driving RMS current*

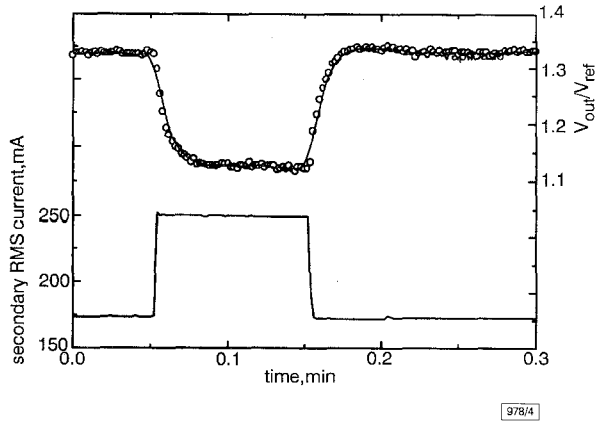

Fig. 4 *Response of sensor (top) to step change of secondary current (bottom)*

electrical current to be measured (I_P) is converted by the CT (a Rogowski coil with a current conversion of 4000:1) to a secondary current (I_s), which is passed directly through the metallic coating of the FBG. Since the reflected Bragg wavelength is dependent on the temperature of the fibre, the I_s^2R heating produced by the secondary current (ranging form 0 to 1A) in the FBG metal coating will shift the Bragg wavelength. By monitoring this shift, the value of the electrical current can be recovered. The Bragg wavelength shift produced is measured using a passive all-fibre demodulation scheme described previously [5]. The biconical fibre filter (BFF) was fabricated with an oscillation period of ~3.5nm and an extinction ratio of ~8.1dB. Over the working range of the FBG (835.9 – 836.8nm) the BFF had a near linear response of ~7dB/nm, as shown in Fig. 2. To measure the wavelength shift of the FBG, and consequently, the secondary electrical current, the ratio of the two detected intensities was implemented by software using the LabView™ program. In this way, compensation is performed for time-varying intensity fluctuations and spectral intensity variations of the broadband source, and also for any coupling loss and microbending fluctuations up to coupler C_2. Fig. 3 shows the sensor output response to a sinusoidal secondary current with frequency 50Hz and driving RMS current ranging from 0.04 to 0.4A. From these results, linearity can be observed throughout the measured region and the obtained data indicates an RMS current resolution of 2mA. It should be pointed out that these results were obtained without the CT and were simulated using a laboratory variable current source with the capability to change the shape, frequency and amplitude of the test current signal applied to the metal-coated FBG. The bandwidth (at –3dB) of the sensor system for a constant RMS current was 2.2Hz. For higher frequencies, the sensor output produced the RMS average of the secondary current waveform, but the DC term cannot easily be distinguished from low frequency drift due to environmental temperature. Fig. 4 shows the response of the sensor to a secondary current step from 175 to 250mA. The time constants for the heating and cooling regimes were (0.46 ± 0.01) and (0.47 ± 0.01)s, respectively, and the AC results give a dynamic sensitivity of ~1mA/√Hz. Nevertheless, it should be possible to increase the frequency response up to tens of kilohertz using a sputtering technique to produce a thinner layer of metal along the FBG. Because CTs are used for both metering (frequency of interest is 50 or 60Hz) and relaying purposes (overload conditions and current spikes), it is also necessary that the frequency response of the sensor system be much higher than the line frequency. Another drawback for this application is the sensitivity of the FBG to the temperature changes induced by both the electric current and by environment fluctuations, which means that some kind of compensation scheme to de-couple the two effects will be necessary. The inherent wavelength encoded output information of these devices make them independent of light levels and good candidates for incorporation into wavelength-division multiplexing schemes. Also, this sensor configuration has the advantage of presenting a purely resistive impedance to the current source.

In summary, a metal-coated fibre Bragg grating sensor for measuring the RMS current of power lines at 50Hz was constructed, providing a resolution of ± 2mA and a dynamic sensitivity of ~1mA/√Hz at 2Hz.

Acknowledgments: P.M. Cavaleiro and A.B. Lobo Ribeiro acknowledge financial support from 'Agência de Inovação' under the HIPOWER project. F.M. Araújo acknowledges support from 'Programa PRAXIS XXI'.

15 April 1998
Electronics Letters Online No: 19980785

P.M. Cavaleiro, F.M. Araújo and A.B. Lobo Ribeiro (*UTOE, INESC - Porto, R. Campo Alegre 687, 4150 Porto, Portugal*)

E-mail: alr@goe.fc.up.pt

A.B. Lobo Ribeiro is also with the Dept. of C&T, Univ. Fernando Pessoa, Pç. 9 Abril 349, 4200 Porto, Portugal

References

1 RASHLEIGH, S.C., and ULRICH, R.: 'Magneto-optic current sensing with birefringent fibres', *Appl. Phys. Lett.*, 1979, **34**, pp. 768–770

2 TANGONAN, G.L., PERSECHINI, D.I., MORRISON, R.J., and WYSOCKI, J.A.: 'Current sensing with metal-coated multimode optical fibres', *Electron. Lett.*, 1980, **16**, pp. 958–959

3 DANDRIDGE, A., TVETEN, A.B., and GIALLORENZI, T.G.: 'Interferometric current sensors using optical fibres', *Electron. Lett.*, 1981, **17**, pp. 523–524

4 FISHER, N.E., HENDERSON, P.J., and JACKSON, D.A.: 'The interrogation of a conventional current transformer using an in-fibre Bragg grating', *Meas. Sci. Technol.*, 1997, **8**, pp. 1080–1084

5 LOBO RIBEIRO, A.B., FERREIRA, L.A., TSEVTKOV, M., and SANTOS, J.L.: 'All-fibre interrogation technique for fibre Bragg sensors using biconical fibre filter', *Electron. Lett.*, 1996, **32**, pp. 382–383

Noise reduction of 20Gbit/s pulse train using spectrally filtered optical solitons

M. Asobe, A. Hirano, Y. Miyamoto, K. Sato, K. Hagimoto and Y. Yamabayashi

It is demonstrated that intensity noise in an optical pulse train can be effectively reduced by the spectral filtering of solitons in an optical fibre.

The 'particle-like' nature of optical solitons is attractive for realising several types of optical functionality. Solitons can propagate, undistorted, over long distances, and their application to long haul optical transmission has been studied intensively [1]. Optical solitons are also useful for optical signal processing, such as all-optical switching. Recently, photon number squeezing has been demonstrated by the spectral filtering of pulses whose intensity is slightly higher than that of the fundamental soliton [2]. This scheme offers a very simple way to reduce the intensity noise of optical pulses. Although sub-shot noise detection has been demonstrated using spectrally filtered solitons, it is not easy to take advantage of the sub-Poissonian state in real optical transmission systems. This is because the photon number in optical communication is far from the ideal shot noise limit for several reasons, one of them being the intrinsic finite noise figure of the widely used Er^{3+}-doped fibre amplifier. However, the spectrally filtered soliton scheme should still be useful for reducing intensity noise caused by intersymbol interference in optical transmitters or amplified spontaneous emission in EDFAs. In this Letter, we demonstrate that the spectrally filtered soliton scheme is effective at improving the signal-to-noise ratio (SNR) of optical communication equipment.

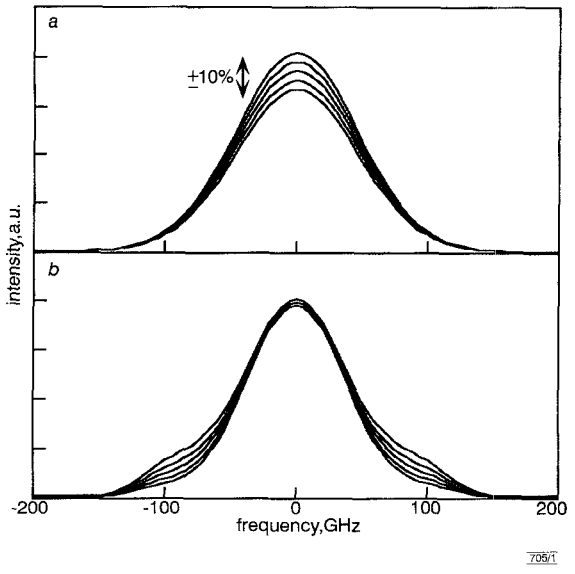

Fig. 1 *Calculated spectra of pulses with intensity variation*

a Input pulse
b Output pulse through optical fibre
T_{FWHM} = 4ps, D = 3.15ps/kmnm, loss = 0.35dB/km, L = 2.91km, N^2 = 1.6, L = 1.32

In the spectrally filtered soliton scheme, optical pulses are injected into an anomalous dispersion fibre and then filtered through a bandpass filter. The key points are that input power is set to be slightly higher than that of the fundamental soliton, and the fibre length is slightly longer than the soliton period. To determine the appropriate experimental conditions, we calculated the nonlinear propagation of the pulse using the split Fourier method [3]. Fig. 1 shows simulated spectra of 4ps wide Gaussian pulses before and after propagation through a 2.9km long fibre. In this case, a group velocity dispersion of +3.15ps/km nm, transmission loss of 0.35dB/km and effective core area of 21μm² were assumed. We also assumed that input peak power has ±10% variation around 183mW, which corresponds to 1.6 times the fundamental soliton power. The fibre length corresponds to 1.3 times the soliton period. As the Figure shows, the spectrum of the pulse is broadened due to self-phase modulation, depending on the intensity of the pulses, but the central part of the spectrum ends up being close to that of a fundamental soliton, so that the difference in the intensity of each pulse is converted to a difference in the spectral wings. The intensity noise can therefore be reduced by eliminating the spectral wings through the use of a bandpass filter. In the case of our estimation, filtering with a bandwidth of ~ 100GHz seems to be effective, as can be seen in Fig. 1.

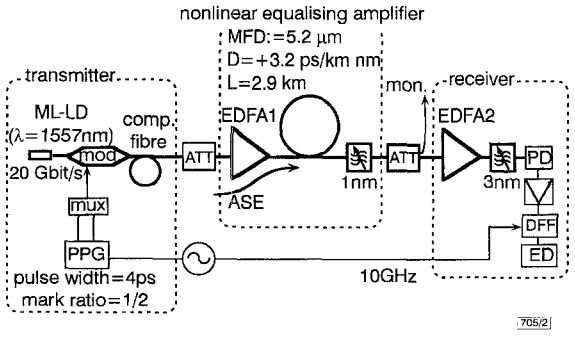

Fig. 2 *Experimental setup*

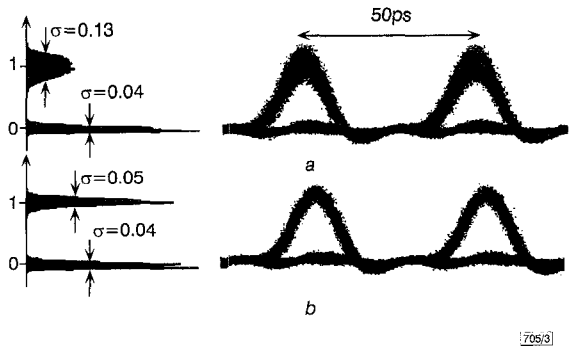

Fig. 3 *Eye diagram and intensity histogram*

a Signal degraded by intersymbolic interference
b Signal processed by spectrally filtered soliton scheme

We conducted several experiments to determine whether this scheme improves the SNR of optical pulses. The experimental setup we used is shown in Fig. 2. The light source was a monolithic modelocked laser diode [4] that generates 6ps wide pulses at a repetition rate of 20GHz. The pulses are encoded by an $LiNbO_3$ modulator at a bit rate of 20Gbit/s with half mark ratio. Residual chirping of the pulses was compensated for by an anomalous dispersion fibre, and this results in 4ps wide pulses. The pulses are amplified by EDFA1 to obtain sufficient power to generate solitons. In some experiments the input power to EDFA1 was attenuated to introduce ASE noise. The amplified pulses are propagated through a 2.9km long dispersion shifted fibre, the group velocity dispersion of which is +3.2ps/km nm. The output is filtered with a bandpass filter (BPF) with a bandwidth of 1nm (FWHM). EDFA1 combined with the soliton fibre and BPF acted as a nonlinear equalising amplifier. The filtered pulses are attenuated and received with a 20Gbit/s receiver, which contains EDFA2, a 3nm BPF, a *pin* photodiode, an electric amplifier, a decision circuit, and an error detector.

To confirm the effect of noise reduction, we prepared a degraded signal by detuning the driving signal to the $LiNbO_3$ modulator. Fig. 3 shows the eye diagram and histogram of the signal before and after soliton noise reduction. The degraded signal possessed a large mark level distribution caused by intersymbol